

# EXPLORATION AND NUMERICAL SIMULATION OF WIND TURBINE WAKE

*F. Massouh\*, I.K. Dobrev\*\**

Ecole Nationale Supérieure d'Arts et Métiers (ENSAM)

bvd. L'Hôpital, 151, Paris, 75013, France

+33 1 44246256/+33 1 44246266;

\*E-mail: fawaz.massouh@paris.ensam.fr

\*\*E-mail: ivan.dobrev@paris.ensam.fr

Received: 24 Sept 2007; accepted: 31 Oct 2007

In this article, the flow behind a horizontal axis wind turbine (HAWT) is investigated and the obtained data is compared to the results of numerical simulation. The aim is to test reliability of random averaged Navier-Stokes (RANS) solver to model the wake behind a wind turbine. The experimental investigations are carried out by means of the 2D PIV measurements. The flow field is obtained in rotating frame of reference in which the rotor appears fixed by means of the phase-locked technique. Explorations are carried out in different azimuth planes. Because of large dimensions of the flow field, each azimuth plane is divided into several windows. For each window, the instantaneous velocity field is measured and stored successively to enable obtaining the averaged velocity field. Then, the flow in each azimuthal plane is reconstructed by stitching the averaged velocity field of these windows. Finally, the 3D velocity field is reconstituted by treating the results of images resulting from the different explored azimuth planes. These results are compared with RANS calculations. In general the numerical results show agreement with experiment, but some inconsistency concerning obtained power is revealed.

**Keywords:** wind energy



*Fawaz Massouh*

**Organization(s):** Ecole Nationale Supérieure d'Arts et Métiers, Researcher, Assoc. Prof.

**Education:** PhD – Paris-VI University (1984).

**Experience:** ENSAM (1979 to now).

**Main range of scientific interests:** fluid mechanics, wind energy.

**Publications:** 7 papers in international scientific journals.



*Ivan Dobrev*

**Organization(s):** Ecole Nationale Supérieure d'Arts et Métiers.

**Education:** Tech. Univ.-Sofia, Faculty of Energetic Machines (1978-1983).

**Experience:** Tech. Univ.-Sofia, assistant (1983-2003). ENSAM, researcher (2004 to now).

**Main range of scientific interests:** wind turbine, aerodynamics.

**Publications:** 2 papers in international scientific journals.

## Introduction

The investigation of the wake development downstream wind turbines is required for the design of wind farms. In this case the wake is influenced by the presence of atmospheric boundary layer, atmosphere instabilities and “ground-wake” interaction. The flow is very complex

and it is very difficult to obtain the velocity field downstream the rotor even with most sophisticated Navier-Stokes solvers. In such case there is need of experimental results that can validate calculations and adjust some parameters. There exist experiments in-situ, which permit to understand the wake structure [1]. However, in the case of large-scale experiments and due

to the sensors applied for velocity measurements, it is difficult to acquire with sufficient spatial and temporal resolution the development of the wake. As results, the usefulness of the obtained velocity field to serve as reference for CFD modeling is limited. Fortunately, there exist investigations of wake flows, which are realized in wind tunnel. These measurements are carried out in controlled flow conditions and more precise methods for the velocity measurement are applied.

Numerous studies were performed in wind tunnels in order to reveal the development of wake behind a wind turbine and to obtain precise results. These studies [2-6] were carried out using a Pitot tube or hot wire anemometry (HWA). The main disadvantage of these experiments is due to one-point measurement capabilities of applied sensors. Thus it is not possible to obtain instantaneous velocity simultaneously in the entire field of investigation. Also, due to limited directional sensibility, it is not possible to obtain the velocities in core of the blade tip vortices. However, the particle image velocimetry (PIV) is a non-intrusive method that permits to measure the instantaneous velocity vectors in plane. But researchers used PIV technique for the exploration of wind turbine wakes are few and their results are rather qualitative. Here we might mention the papers [7-12]. Recently, stereo PIV measurements are carried in out the case of HAWT with diameter of 4.5m and first results are published in [13].

The aim of this study is to present the quantitative information about the wake downstream of model wind turbine. This information is acquired by means of the PIV technique and cannot be obtained by techniques of HWA or pneumatic sensors. For example, the possibility of obtaining numerical data on velocity field around the tip vortices is of great interest. Moreover, the quality of data obtained in case of yaw and non-yaw flow conditions permits to use these results as reference in case of CFD computing of flow around the model wind turbine. Finally in this study, the numerical simulation is carried out in the case of non-yaw conditions. The comparison of obtained results with experiment permits to reveal some particularities of the used random averaged Navier-Stokes (RANS) solver.

### Experimental results

The Fluid Mechanics Laboratory at ENSAM, Paris has a closed circuit wind tunnel with a semi-open test section. A settling chamber is equipped with a convergent nozzle which has contraction ratio of 12. This contraction ratio ensures a uniform flow and the turbulence intensity does not exceed 0.5 % for a velocity of 35 m/s. The test section has working dimensions 1.35 m by 1.65 m and 2 m of length. The investigation is carried out in wind tunnel using a modified commercial wind turbine Rutland 503.

This horizontal axis wind turbine has a three blade rotor with diameter of 500 mm and hub diameter of 135 mm. The blades are tapered and untwisted. They have a pitch

angle of  $10^\circ$  and a chord of 45 mm at tip and 65 mm at the root. The rotational speed is 1000 rpm with a free-stream velocity of 9.3 m/s. Hence, the TSR is equal to 3, which is lower than the case of market wind turbines. The wind turbine is mounted on a support tube of 37 mm of diameter ensuring a sufficient height in order to allow the lasers fixed above the transparent roof to illuminate the explored plane with a sufficient intensity, Fig. 1.

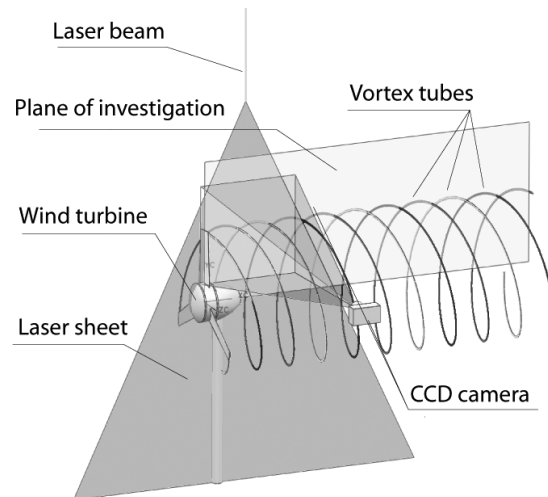


*Fig. 1. Experimental test bench*

The PIV technique is applied to obtain the velocity field in the wake downstream the turbine rotor. Here, a double cavity Quantel “Blue Sky” Nd:YAG pulsed laser (532 nm), which produce approximately 120 mJ per pulse, is installed above the transparent roof of the wind tunnel test section. A cylindrical lens is used to create a thin vertical sheet of laser light, which passes through the center of the rotor. As the test section is semi-open and without sidewalls, it is possible to place the camera outside the tunnel, Fig. 1. Olive oil droplets are introduced for seeding on the inlet of the wind tunnel diffuser.

In order to carry out the phase-locked measurements, the test bench is equipped with an optical sensor. This sensor synchronize the lasers pulses and a reference angular position of the blade. The sensor tracks a reflecting target fixed on the rotor hub and emits a signal, each time when the target passes. Then the emitted signal is sent via a delay circuit. The change of delay time permits to change the angular distance between the reference position of blade and the plane of exploration.

As the plane of exploration passes trough the rotor axis and the PIV used in this study is planar, then it is only possible to obtain radial and axial velocities. However the tangential velocity of the flow downstream the rotor is not zero and time interval between two laser pulses is set to 150  $\mu$ s, it is probable that the tracked particles will be blown out of the illuminated volume. Therefore, it is needed to adjust the laser sheet thickness to nearly 3-4 mm.

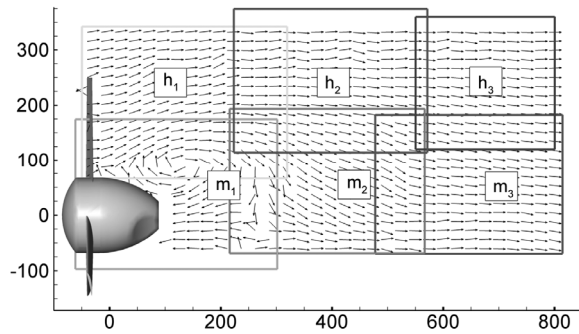


Fig. 2. Flow map reconstruction

Exploration of flow downstream the rotor is carried out in four azimuth planes with angles  $0^\circ$ ,  $30^\circ$ ,  $60^\circ$  and  $90^\circ$ . Here, the plane of  $0^\circ$  corresponds to the vertical position of the reference blade, Fig. 2. Because of the laser output power limitation and the camera resolution of  $1600 \times 1200$  pixels, it is not possible to obtain with sufficient precision a velocity field larger than 300 mm. As a consequence to widen the explored area, the investigated velocity field is divided into six windows (3 horizontal by 2 vertical) with a certain overlapping. The scale of windows and their relative positions are defined using calibration markers placed in known positions inside the interrogation area. For this purpose, the images of these markers are taken after each series of tests.

For each explored window the imagery is repeated 95 times synchronously with rotor rotation. Hence temporal sequence is acquired during approximately 12 seconds in order to improve the precision of averaged velocity calculation.

Totally, four series of 6 by 95 pairs of images were acquired for different planes with azimuth angles of  $0^\circ$ ,  $30^\circ$ ,  $60^\circ$  and  $90^\circ$ ; with zero corresponding to the vertical position of the reference blade.

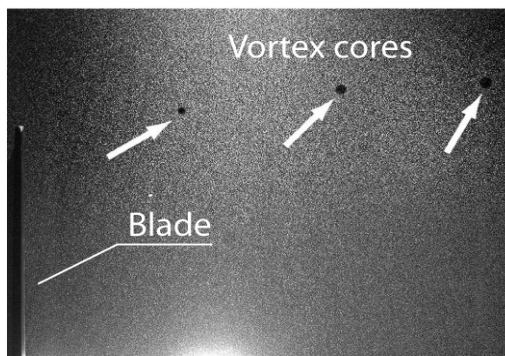


Fig. 3. Raw image taken immediately behind the rotor in the h1 window

The raw images have a resolution of  $1600 \times 1200$  pixels and 12 bits of grayscale resolution. Thanks to the synchronization between the laser pulse and the rotor position detected by the optical sensor, we can distinguish a blade frozen in vertical position, on the left. It can be seen also the cores of vortex tubes emitted from

the tips of other blades, Fig. 3. Due to velocities induced by these vortices the seeding particles are turned around the vortex core center and the centrifugal forces carry out these particles outside of the vortex center. As results the vortex tube core appears on the images like a black spot because the quantity of the seeding particles decreases inside.

Statistical processing of the raw images is carried out by means of Matpiv ver.1.6.1 developed by Sveen [14]. The “multi-pass” algorithm with 3 pass is applied, the final size of interrogation window is  $16 \times 16$  pixels and the overlapping is 75 %. The obtained results are filtered by means of signal-to-noise (SNR), median and mean filter, then all vectors marked as “spurious” are discarded and new values are obtained by interpolation from nearest points. The criterion for discarding is the quality of velocity and vorticity fields. If the level of cut-off SNR is too high the flow is smoothed and some vorticity structures disappear, but if the SNR is too low then vorticity field is very noisy. Then instantaneous velocity fields resulting from each time series of 95 captured images are used to obtain the average fields in each of the investigated windows. Finally, the processing of the calibrating images makes it possible to obtain the scale constants, true velocity and the position of each window relative to the rotor. In this manner the fields of instantaneous and averaged velocity are calculated for each window.

Some uncertainty on the velocity measurement in the vicinity of the blade comes from the specific difficulties of the PIV technique to explore flow field close to the walls due to reflection. It must be noted also, that the high levels of the tangential velocities can take place just a few millimeters from the blades. This does not permits that the same seeding particles remain in the laser sheet between consecutive laser pulses. As result, the cross-correlation algorithm used in PIV image analysis fails to obtain the instantaneous velocity field.

The Fig. 4 shows the field, which results from averaged velocity fields for windows h1. Here, it can be observed the intersection between the plane of exploration defined by the laser sheet and the helical vortex tubes emanating from blade tips. Also it can be seen the effect of flow deceleration created by the wind turbine rotor whose consequence is shown by the increase of the downstream flow tube diameter. It must be noted that the flow tube is not cylindrical as assumed in the linear theory of propellers. We clearly see the deformation of flow tube surface due to the presence of tip vortices. It should be noted that there is a large vortex structure, which results from a detachment behind the hub. In the vicinity of the blade, the flow field is not well resolved, because of the presence of walls.

The analysis of near rotor wake shows that the hub is a major source of disturbances and unsteady aerodynamic effects. This is due to the bluff shape of the rotor hub, which contains the electric generator. The flow detachment from the hub is intensified due to the highly loaded root blade sections. For this reason high axial

velocities are induced; the flow on the hub surface is decelerated and then separated in vicinity of the blade attachment to the hub. The results of this phenomenon are visible in Fig. 4 where we note a return flow up to approximately 40 % of the diameter of the rotor.

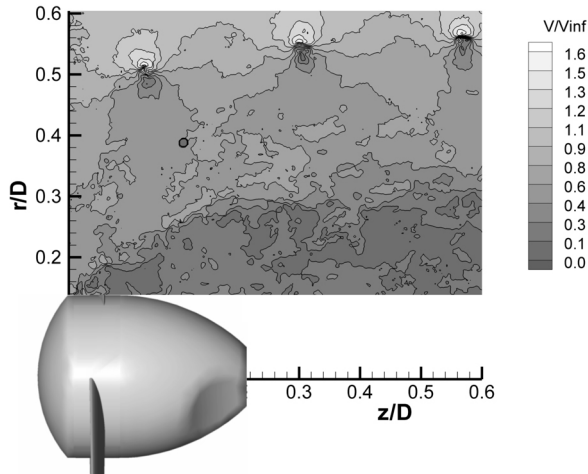


Fig. 4. Contours and vectors of average velocity in  $h1$

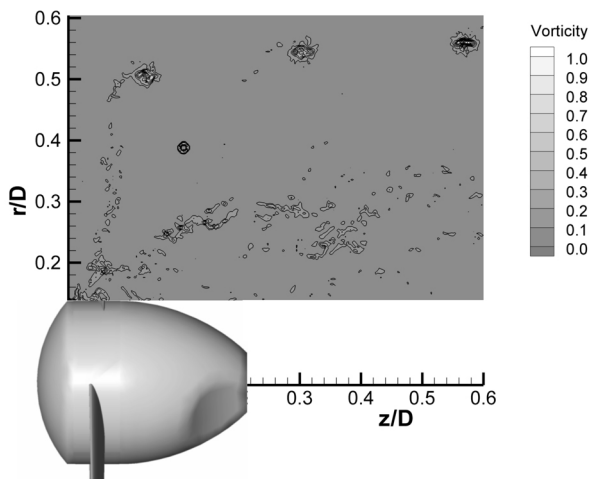


Fig. 5. Vorticity of instantaneous velocity in  $h1$  window

The investigation of the time series of instantaneous vorticity fields, Fig. 5, shows that there is a fluctuation in the position of the cores of the tip vortices. These fluctuations, known as vortex wandering, produce an artificial reduction of vortex intensity when the average values are calculated from the instantaneous fields. The fluctuation of vortex center behind the rotor is shown on Fig. 6. It can be observed that the amplitude of the fluctuations increases downstream the rotor. In reality, in spite of vortex position instability, the vortex intensity and vortex core velocity does not decrease not as rapidly, see Fig. 7 and Fig. 8, as the averaged velocity field predict. Consequently, the average velocity field is not completely representative for comparison with steady numerical simulations.

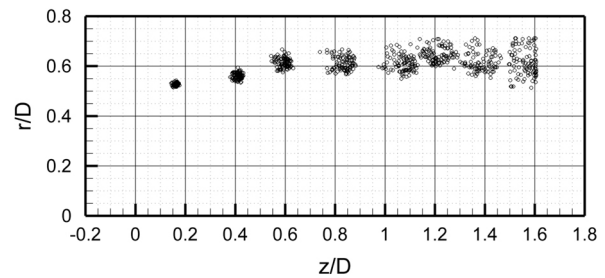


Fig. 6. Vortex wandering behind the rotor

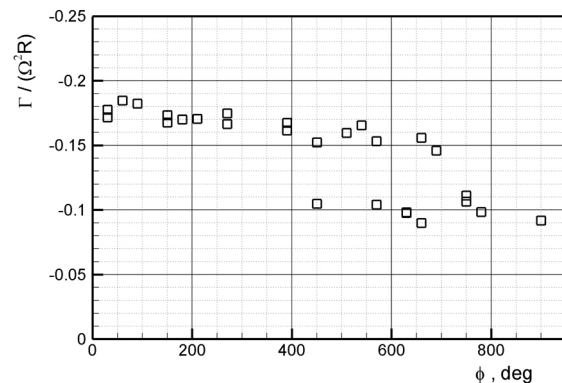


Fig. 7. Vortex intensity behind the rotor

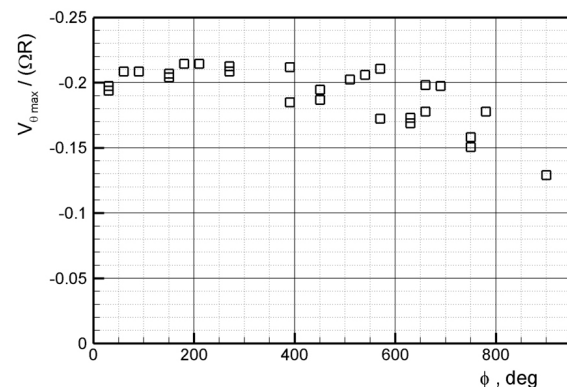


Fig. 8. Vortex core maximum velocity

### Numerical simulation

To investigate flow downstream the rotor a computational analysis is carried out using commercial CFD code Fluent 6.3. In this simulation the rotational periodicity is not used and the flow past the rotor is modeled completely and not only one period. The periodicity is not used because this improves the unsteady simulation. In order to model the flow blockage the rotor is modeled as it rotates in the wind tunnel. Therefore, the tunnel walls are modeled to confine the flow about the rotor and this creates more realistic induced velocities. Because CFD Fluent does not support chimera grid, the blade rotation around the rotor axis is modeled using a sliding mesh technique. Hence, the flow field is divided in two distinct cell zones; one that represents the wind

tunnel and other that represents the turbine rotor. In Fluent, these adjacent cell zones are associated to form three grid interfaces.

During the calculation, the cell zones rotate relative to one another along the grid interface in discrete steps. The cylinder, which represents the rotor and includes the blades, has the diameter  $1.5D$  and the length  $0.4D$ . In order to create a more regular grid around the suction and pressure surfaces of the blades, the rotor domain is divided along the blades by means of three parallelepipeds. Then the internal volume is divided once again in four sectors. Finally, the hexagonal volumes that include the pressure and suction surfaces blade surfaces are meshed using the hexagonal cells structured grid, Fig. 9.

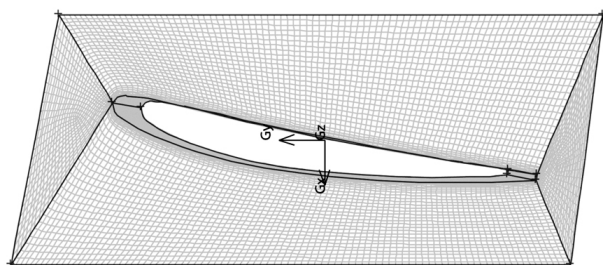


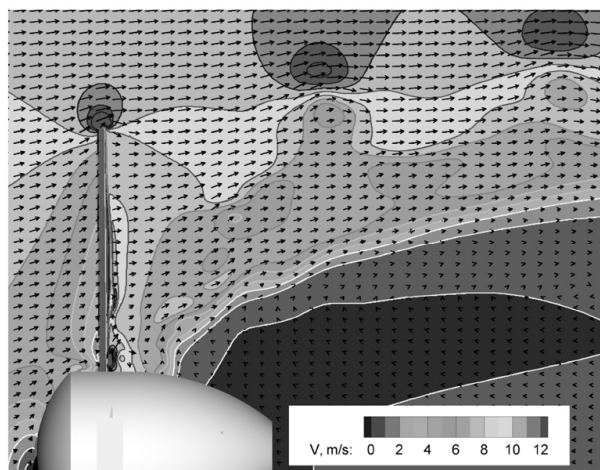
Fig. 9. Grid blocks around the blade

The blade suction and pressure surfaces are divided in the chordwise direction into 90 intervals, which are slightly refined near the leading and trailing edges where the velocity gradient is strongest. In spanwise direction the blade is divided into 90 intervals equally spaced. In order to improve the mesh in the boundary layer, 10 mesh layers in vicinity of blade walls are used. Here, the initial cells size in normal direction is 0.15 percent of

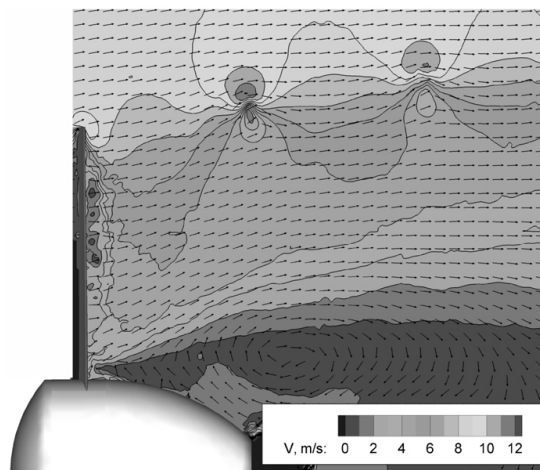
chord lengths and the growth factor of 1.25 is used. Totally 6 million hexahedral cells are used in rotor grid zone. To model the wind tunnel a multi-block grid of 10 hexahedral million cells is used. In order to decrease the cell number on tunnel walls we specify a wall shear stress of 0 Pa, so there is no need of boundary layer modeling. To compute this model divided in 8 partitions we employ a cluster of 4 PC with Pentium IV processors of 3.4 GHz and 4 GB of RAM each.

The Reynolds number of the blade tip sections is near 70,000. For this reason the turbulence model used is  $k-\omega$  Shear Stress Transport (SST) which is considered to be more robust than others low-Reynolds number  $k-\omega$  or standard  $k-\epsilon$  models. This model employs a standard  $k-\omega$  model in the inner region of the boundary layer, and a high-Reynolds number  $k-\epsilon$  model in the rest. For the “pressure-velocity” coupling we use the SIMPLE algorithm and a second-order upwind differencing discretization scheme for the momentum equations. The time step is equivalent to a blade rotation of  $1^\circ$  about the rotor axis; each time step has 10 iterations and the results repeatability is obtained after 3 rotor turns.

In general the obtained results by Fluent correspond to experimental values. Unfortunately, it is seen that vortex core radii are lower and the distance between vortex cores is greater compared to experimental results, Fig. 10. This is due to the fact that the obtained power is lower. Also it must be noted that the flow separation downstream the rotor hub is strongest. This is a consequence of the RANS models failure to predict the flow separation. For regret, the other turbulence models, for example RSM or V2F also do not allow to obtain more realistic results for flow downstream of the rotor. Probably, to obtain better results it is necessary to use LES or DES model.



a



b

Fig. 10. Velocity field downstream rotor obtained by simulation (a) and by experiment (b)

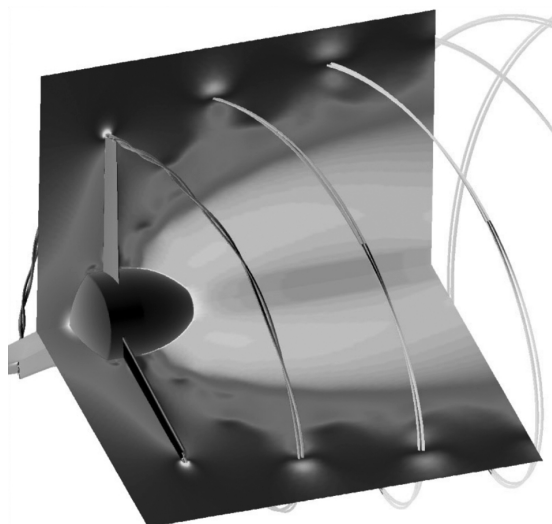


**Fig. 11.** Velocity field and vortex tube issued from the blade tip

### Conclusion

In the present study, the PIV technique is successfully applied for investigation of the wake behind a horizontal axis wind turbine. The phase-locked measurements are applied and the images retrieval is synchronized with azimuth position of the blade. This permits to carry out flow measurements in the reference frame of the rotor and makes possible to reconstruct the 3D velocity field of the wake. To widen the measured field, the azimuthal plane of exploration is divided into 6 windows with some overlap. Then, by means of the position markers, these windows are stitched and the velocity field in the complete plane is obtained. Thus, the helical pitch and the radial position of the tip vortices, compared to the rotor, can be localized.

The results show that the radius of the tip vortices issued from the blade tips is not constant as it is assumed in linear propeller theory. In reality, the diameter of the flow tube increases as the simple theory of Froude-Rankine predicts it. Measurements revealed also the presence of important vortex structures downstream the hub and near the root of the blade. Some instability of the helical tip vortices, so called vortex wandering is also to be noted. Because of these fluctuations, the instantaneous velocity field is very rich with information. The numerical data concerning the instantaneous field constitutes a useful database for the validation of models of wind turbine rotors and the prediction of near wake development.

The RANS calculation is carried out in order to show a potential of numerical simulation of the flow behind the wind turbine. From the computation results presented above, it can be seen that the obtained CFD results show good agreement with experiments. However, there are some discrepancy due to incapability of CFD to resolve well the detached flows and also the need to introduce a transition model.

### References

1. Vermeer L.J., Sorensen J.N., Crespo A. Wind turbine wake aerodynamics // Progress in Aerospace Sciences. 2003. Vol. 39. P. 467–510.
2. Massouh F., Dobrev I., Dejean F., Laborie A. Etude du sillage d'une éolienne à axe horizontal. 16ème Congrès Français de Mécanique CFM 2003, Nice, 2003.
3. Vermeer L.J. A review of wind turbine wake research at TU Delt, 2001 AIAA paper 2001-0030.
4. Ebert P.R., Wood D.H. The near wake of a model horizontal axis wind turbine-I. Experimental arrangements and initial results // Renewable Energy. 1997. Vol. 12, No. 3. P. 225-243.
5. Ebert P.R., Wood D.H. The near wake of a model horizontal axis wind turbine – Part 3: properties of tip and hub vortices // Renewable Energy. 2001. Vol. 22. P. 471-472.
6. Massouh F., Dobrev I. Investigation of wind turbine near wake. Int. Conf. on Jets, Wakes and Separated Flows, ICJWSF-2005, Toba-shi, Mie, Japan, Oct. 5-8, 2005.
7. Mast E.H.M., Vermeer L.J., van Bussel G.J.W. Estimation on the circulation distribution on a rotor blade from detailed near wake velocities // Wind Energy. 2004. Vol. 7. P. 189-209.
8. Grant I., Parkin P., Wang X. Optical vortex tracking studies of a horizontal axis wind turbine in yaw using laser-sheet flow visualization // Experiments in Fluids. 1997. Vol. 23. P. 513-519.
9. Grant I., Parkin P. A DPIV study of the trailing vortex elements from the blades of a horizontal axis wind turbine in yaw // Experiments in Fluids. 2000. Vol. 28. P. 368-376.
10. Grant I., Mo M., Pan X., Parkin P., Powell J., Reinecke H., Shuang K., Coton F., Lee F. and D. An experimental and numerical study of the vortex filaments in the wake of an operational horizontal-axis wind turbine // Journal of Wind Engineering and Industrial Aerodynamics. 2000. Vol. 85. P. 177-189.
11. Whale J., Helms C., Papadopolous K.H., Anderson C.G., Skyner D.J. A study of the near wake structure of a wind turbine comparing measurements from laboratory and full-scale experiments // Solar Energy. 1996. Vol. 56, No. 6. P. 621-633.
12. Maeda T., Kinpara Y., Kakinaga T. Wind tunnel and field experiments on wake behind horizontal axis wind turbine // Trans. of Jap. Soc. Mec. Eng. 2005. Vol. 71, No. 701. P. 162-170.
13. The MEXICO project: Snel, Shepers J.G. and Montgomerie H. The database and first results on data processing and interpretation // Journal of Physics: Conference Series. 2007. Vol. 75.
14. Sveen J.K., Cowen E.A. Quantitative imaging techniques and their application to wavy flows, in PIV and Water Waves, editors J. Grue, P.L.F. Liu and G. Pedersen // World Scientific. 2004.

